Rapid Communications

Observation of dipolar splittings in high-resolution atom-loss spectroscopy of ^{6}Li p-wave Feshbach resonances

Manuel Gerken,[1] Binh Tran,[1] Stephan Häfner,[1] Eberhard Tiemann,[2] Bing Zhu,[1,3,*] and Matthias Weidemüller[1,3,†]

[1]*Physikalisches Institut, Universität Heidelberg, Im Neuenheimer Feld 226, 69120 Heidelberg, Germany*

[2]*Institut für Quantenoptik, Leibniz Universität Hannover, Welfengarten 1, 30167 Hannover, Germany*

[3]*Hefei National Laboratory for Physical Sciences at the Microscale and Department of Modern Physics, and CAS Center for Excellence and Synergetic Innovation Center in Quantum Information and Quantum Physics, University of Science and Technology of China, Hefei, Anhui 230026, China*

(Received 20 September 2019; published 11 November 2019)

We report on the observation of dipolar splitting in ^{6}Li p-wave Feshbach resonances by high-resolution atom-loss spectroscopy. The Feshbach resonances at 159, 185, and 215 G exhibit a doublet structure of 10, 6, and 13 mG, respectively, associated with different projections of the orbital angular momentum. The observed splittings agree well with coupled-channel calculations. We map out the temperature dependence of the atom-loss spectrum and extrapolate resonance positions as well as the corresponding widths to zero temperature. The observed dipolar splitting in fermionic lithium might be useful for the realization of the quantum phase transition between the polar and axial p-wave superfluid phases.

DOI: 10.1103/PhysRevA.100.050701

I. INTRODUCTION

It is generally known that magnetic p-wave Feshbach resonances (FRs) in ultracold atomic collisions exhibit a dipolar splitting, resulting in two resonance features corresponding to $m_l = 0$ and $|m_l| = 1$ [1,2]. Here, m_l is the projection of the orbital angular momentum l along the external magnetic field. This nondegeneracy was predicted to give rise to a phase transition from a p_x to a $p_x + ip_y$ state in a p-wave superfluid (SF) [3], which plays an essential role in SF liquid ^{3}He [4] and neutron SFs inside neutron stars [5,6]. The dipolar splitting was observed in a spin-polarized gas of ^{40}K [1] and a large variety of quantum-gas mixtures [7–12]. It is attributed to effective spin-spin (ss) interactions including the magnetic dipole-dipole interaction and the second-order spin-orbit coupling [2]. Recently, the observation of dipolar splitting has been extended to d-wave resonances [13,14], and an additional splitting mechanism has been discovered for $m_l = +1$ and $m_l = -1$ due to the spin-rotation interaction in p-wave FRs [15,16].

Due to the favorable properties of its FRs, the fermionic isotope of lithium, ^{6}Li, one of the only two stable fermionic isotopes among the alkali metals, has been a major workhorse in experiments with quantum-degenerate Fermi gases. Prime applications include the study of the BCS-BEC crossover [17–23], the Efimov effect [24–28], the double SF [29], and the Fermi-Hubbard model in optical lattices [30–35]. Although dipolar splitting in ^{6}Li p-wave FRs was predicted to be ∼10 mG [36], it was not resolved so far due to insufficient magnetic resolution in previous experiments [37–42]. By using an optical lattice, p-wave Feshbach molecules in the $|m_l| = 1$ component were selectively formed without resolving the dipolar splitting [43], while the studies of the molecular binding energy and lifetime in Refs. [44–46] neglected this effect.

In this Rapid Communication we report high-resolution trap-loss spectroscopy on three ^{6}Li p-wave FRs in the two lowest-energy hyperfine states. Dipolar splittings of about 10 mG are resolved in all three resonances and systematic effects of the sample temperature on the observed splitting are investigated. We model the observations with a coupled-channel (CC) calculation and find an excellent agreement between experiment and modeling.

II. DIPOLAR SPLITTING

A detailed description of our experimental apparatus has already been given in previous publications [9,47]. In brief, we optically trap a laser-cooled sample of ^{6}Li atoms in the two energetically lowest hyperfine states $|f = 1/2, m_f = 1/2\rangle$ (labeled as $|1\rangle$) and $|f = 1/2, m_f = -1/2\rangle$ (labeled as $|2\rangle$) in a cigar-shaped optical dipole trap. Here, f and m_f refer to the total angular momentum and its projection along the external magnetic field. The sample is evaporatively cooled within ∼5 s at a magnetic field of ∼890 G. Both spin states can be selectively populated by removing the other one with a short resonant light pulse. Finally, we end up with 3×10^4 atoms in each spin state at a temperature of $T \approx 0.14\ \mu$K. The trapping frequencies are determined to be $\omega = 2\pi \times (30, 170, 180)$ Hz, resulting in a peak atomic density of $1.6(1) \times 10^{11}$ cm^{-3} and $T/T_F = 0.53(4)$.

Three ^{6}Li p-wave FRs are identified by performing magnetic-field-dependent loss spectroscopy of Li samples either polarized at a single hyperfine state ($|1\rangle$ or $|2\rangle$) or in a

*bzhu@physi.uni-heidelberg.de
†weidemueller@uni-heidelberg.de

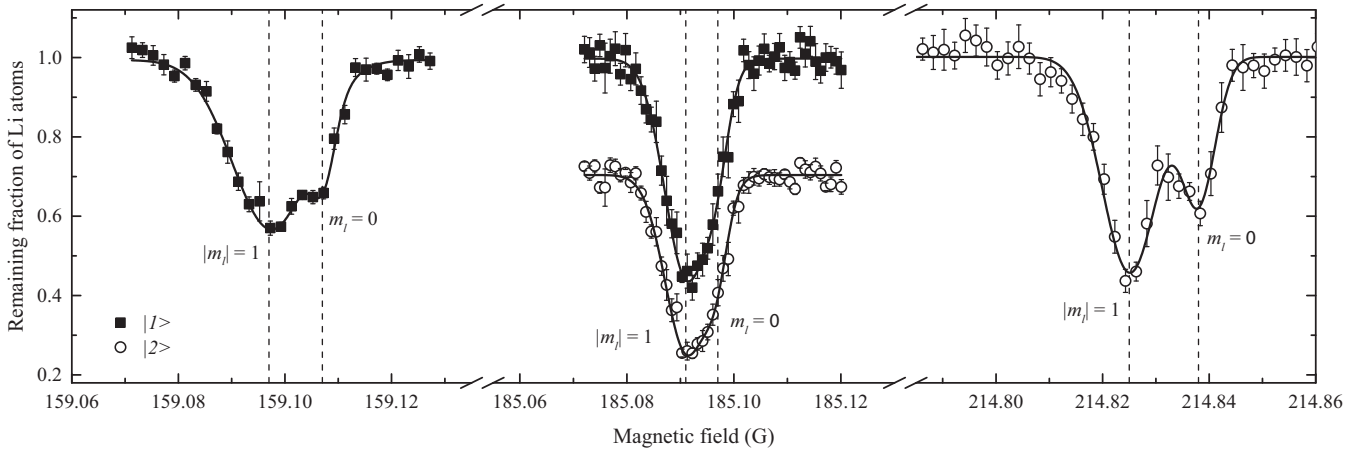

FIG. 1. ^{6}Li p-wave FRs in the $|1\rangle \oplus |1\rangle$, $|1\rangle \oplus |2\rangle$, and $|2\rangle \oplus |2\rangle$ entrance channels observed as atomic-loss features. The figure shows the fractional remaining Li atoms in spin-state $|1\rangle$ (solid squares) or $|2\rangle$ (open circles) after a holding time of 500, 150, and 100 ms from left to right, respectively. All three resonances show doublet structures, where quantum numbers m_l are assigned according to theoretical modeling. The data of spin-state $|2\rangle$ for the resonance near 185 G is vertically shifted to avoid overlapping with that of $|1\rangle$. The solid curves are fits of multipeak Gaussian functions from which the resonance positions B^e (indicated by vertical dashed lines) and widths w^e are extracted as listed in Table I.

mixture of both spin states, as shown in Fig. 1. After optimized holding times of 500 ms (159 G FR), 150 ms (185 G FR), and 100 ms (214 G FR), the remaining number of Li atoms in each spin state is detected by absorption imaging. The points for each resonance are taken in a random order of the magnetic field. Calibration of the magnetic field is performed by rf spectroscopy of the nuclear spin-flip transition between the Li $|1\rangle$ and $|2\rangle$ state. The Breit-Rabi formula is then used to infer the magnetic field strength. Its total uncertainty is derived from calibration measurements to be 10 mG, resulting mainly from day-to-day drifts, with a small contribution from the residual field curvature along the long axis of the atom cloud ($\sim$2 mG), and calibration uncertainties.

In Fig. 1, doublet structures corresponding to $|m_l| = 1$ and $m_l = 0$ components in the ^{6}Li p-wave FRs are presented. Gaussian functions are fitted to the data to extract the loss peak positions $B^e_{|m_l|}$ and loss widths $w^e_{|m_l|}$ (full width at half maximum). For the resonance near 185 G, the positions are assumed to have the same value for both spin states while the widths and amplitudes are fitted independently [48]. Doublet splittings are defined as $\delta^e = B^e_0 - B^e_1$, the distances between the two peaks. We find splittings of 10(1), 6(1), and 13(1) mG for the 159-, 185-, and 214-G p-wave FR, respectively.

The results are listed together with the theoretical resonance splitting δ^t obtained from a full CC calculation in Table I. The assignments of quantum numbers m_l in Fig. 1 are from the CC calculation. The observed doublet splittings are in very good agreement with a CC calculation including an effective spin-spin interaction, similar to the procedure in Ref. [49]. Our observations agree very well with previous predictions [36,44].

TABLE I. ^{6}Li p-wave FRs. The experimentally obtained resonance positions B^e_1, doublet splittings δ^e, and widths $w^e_{|m_l|}$ are extracted by fitting multipeak Gaussian functions to the loss spectra. For the 185-G resonance fitting results of both spin states are listed (the upper row for $|1\rangle$ and the lower one for $|2\rangle$). The first number in parentheses gives their determination uncertainty and the second number the systematic uncertainty of 10 mG. The theoretical doublet splittings δ^t obtained from the CC scattering calculations for a relative kinetic energy of $k_B \times 140$ nK, matching with the experimentally measured temperature, are given.

	B^e_1 (G)	w^e_0 (mG)	w^e_1 (mG)	δ^e (mG)	δ^t (mG)
$\|1\rangle \oplus \|1\rangle$	159.097(1)(10)	6(2)	17(2)	10(1)	10
$\|1\rangle \oplus \|2\rangle$	185.091(1)(10)	10(1)	5(2)	6(1)	4
	185.091(1)(10)	9(1)	5(1)	6(1)	4
$\|2\rangle \oplus \|2\rangle$	214.825(1)(10)	7(2)	10(1)	13(1)	13

III. EFFECTS OF FINITE TEMPERATURE

The finite temperature of the gas causes systematic effects on Feshbach resonances in atom-loss spectra, such as asymmetries, shifts, broadenings, and saturation [1,11,37,41,42]. Averaging over the Maxwell-Boltzmann distribution of the collision energy results in an asymmetric line shape [1,36] shifting the resonance center and broadening the spectrum. Saturation of atom loss stems from the unitarity limit at finite temperatures, rendering it impossible to resolve magnetic resonance splittings below magnetic fields of order $3k_BT/2\delta\mu$ [41,42], with $\delta\mu$ denoting the relative magnetic moment between the molecular and atomic states. To ensure that our measurements (magnetic field resolution of $\sim$1 mG) are not limited by such effects, temperatures below $T \sim 0.7$ μK near the 214-G resonance [$\delta\mu = k_B \times 118(8)$ μK/G [44]] are required.

We investigate the temperature effects on the resonance line shapes near the 214-G p-wave FR.

Evaporation is stopped at varying trap depths resulting in $T \leqslant 0.3$ μK, and atomic-loss spectra are recorded, as shown in Fig. 2(a). Above 0.3 μK the line shape becomes asymmetric and the doublet spitting is unresolvable due to the increase

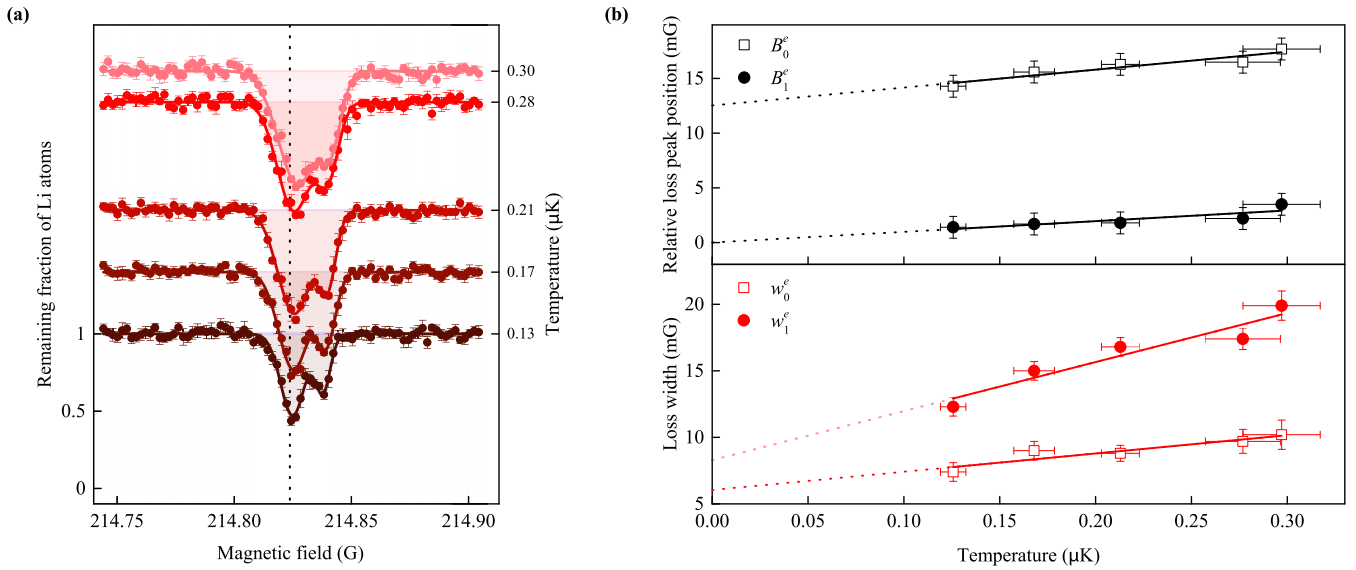

FIG. 2. Temperature dependence of trap-loss spectrum near the 214-G ^{6}Li p-wave FR. (a) Loss spectrum at different sample temperatures. The baselines of the profiles are shifted according to T, as shown at the right axis. The data are fitted using a double-Gaussian function to extract the loss peak positions $B^e_{m_l}$ and widths $w^e_{|m_l|}$. The dotted vertical line shows the extrapolated peak position of B^e_1 at zero temperature at 214.824 G. (b) $B^e_{|m_l|}$ (black symbols) and $w^e_{|m_l|}$ (red symbols) of the observed loss features at different T for the $|m_l| = 1$ (solid circles) and $m_l = 0$ (open squares) components. $B^e_{|m_l|}$ are referenced to the zero-temperature value of B^e_1 at 214.824 G. The lines are linear fits to the data.

of both the temperature-broadened width and the influence of effects due to unitarity, as discussed above. The extracted loss peak positions and widths are plotted in Fig. 2(b).

As expected [1], the resonance peak moves towards a lower magnetic field at a lower temperature. We notice that the observed loss width w^e is considerably larger than the expected temperature-broadened width $k_BT/\delta\mu$, ranging between 1.1 and 2.5 mG within the temperature range of the experiments. To the lowest order, the observed temperature dependence of the loss peak position and width can be well approximated by linear functions [black and red lines in Fig. 2(b)]. This yields for the resonance positions slopes of 16(3) and 10(3) mG/μK for the $m_l = 0$ and $|m_l| = 1$ components, respectively. Although the slopes are slightly different for the two $|m_l|$ values, the doublet splitting δ^e remains almost constant within the experimental uncertainty when T is varied. Extrapolation to zero temperature gives a splitting of 13(1) mG.

Using the Breit-Wigner theoretical approach described in Refs. [41,42] and assuming k_BT as the smallest energy scale, we have estimated the shift of the resonances for two- and three-body loss processes to be $5k_B/2\delta\mu = 21.2$ mG/μK and $k_B/\delta\mu = 8.5$ mG/μK, respectively. By comparing the experimental and theoretical slopes we infer that both two- and three-body loss contributes to the observed temperature dependence. Disentangling these loss channels by time-resolved measurements is beyond the scope of this Rapid Communication. In order to realize a p-wave SF, one would have to mitigate loss by identifying appropriate temperature and density regimes, or by using dimensional control [41,50].

For the observed widths of the loss resonances, we obtain slopes of 37(7) and 14(4) mG/μK for the $|m_l| = 1$ and $m_l = 0$ components, while the zero-temperature widths are 8(1) and 6(1) mG, respectively. Contributions to the observed widths include the resonance intrinsic width γ [36,41,42], the thermal broadening, and other experimental broadening effects such as the trap-induced density inhomogeneity, magnetic field noise, and the hold time. From the observation in Fig. 2(b) [$w^e(T) > k_BT/\delta\mu$] one may infer that $\gamma \gg k_BT$ in our experiment. This conclusion, however, is in disagreement with recent estimations of γ extracted from the temperature- and interaction-strength-dependent two- [41] and three-body [42] loss rate constants near the p-wave resonances above the Fermi temperature.

IV. CONCLUSION

In conclusion, we have performed high-resolution atom-loss spectroscopy of p-wave Feshbach resonances in an optically trapped ultracold ^{6}Li gas and resolved the splittings of about 10 mG between $m_l = 0$ and $|m_l| = 1$ components. Our measurements agree excellently with a full CC calculation including spin-spin interactions.

In spin-polarized Fermi gases near p-wave FRs, there have been predictions of the phase transition from a polar p_x state to an axial $p_x + ip_y$ state as well as the topological transition from a gapless to a gapped $p_x + ip_y$ phase [51–53]. In the past, the stabilities of single-component Fermi gases and p-wave Feshbach molecules near p-wave FRs were investigated, while the realization of p-wave SF in quantum gases is still challenging due to severe inelastic losses [37,38,44–46,54,55]. Dimensional confining has been identified as a promising route for stabilizing Fermi gases near p-wave FRs and realizing p-wave SF pairing [41,50]. Resolving the predicted dipolar splitting of FRs in ^{6}Li provides a good starting point for future investigations in this direction exploring the individual control of $|m_l| = 0, 1$ scattering processes [56,57]. Furthermore, experimental studies of the p-wave contact can now be extended to ^{6}Li, which was previously only accessible in a ^{40}K gas due to its larger splitting of the m_l components [58].

ACKNOWLEDGMENTS

We are grateful to J. Ulmanis, S. Jochim, and S. Kokkelmans for inspiring discussions. S.H. acknowledges support by the IMPRS-QD. This work is supported in part by the Heidelberg Center for Quantum Dynamics, the DFG/FWF Research Unit FOR2247 under Project No. WE2661/11-1, and the DFG Collaborative Research Centre SFB1225 (ISOQUANT).

[1] C. Ticknor, C. A. Regal, D. S. Jin, and J. L. Bohn, Phys. Rev. A **69**, 042712 (2004).
[2] C. Strauss, T. Takekoshi, F. Lang, K. Winkler, R. Grimm, J. Hecker Denschlag, and E. Tiemann, Phys. Rev. A **82**, 052514 (2010).
[3] V. Gurarie and L. Radzihovsky, Ann. Phys. **322**, 2 (2007).
[4] G. E. Volovik, *Exotic Properties of Superfluid* ^3He (World Scientific, Singapore, 1992), Vol. 1.
[5] D. Page, M. Prakash, J. M. Lattimer, and A. W. Steiner, Phys. Rev. Lett. **106**, 081101 (2011).
[6] P. S. Shternin, D. G. Yakovlev, C. O. Heinke, W. C. Ho, and D. J. Patnaude, Mon. Not. R. Astron. Soc.: Lett. **412**, L108 (2011).
[7] K. Pilch, A. D. Lange, A. Prantner, G. Kerner, F. Ferlaino, H.-C. Nägerl, and R. Grimm, Phys. Rev. A **79**, 042718 (2009).
[8] P.-J. Wang, Z.-K. Fu, S.-J. Chai, and J. Zhang, Chin. Phys. B **20**, 103401 (2011).
[9] M. Repp, R. Pires, J. Ulmanis, R. Heck, E. D. Kuhnle, M. Weidemüller, and E. Tiemann, Phys. Rev. A **87**, 010701(R) (2013).
[10] F. Wang, D. Xiong, X. Li, D. Wang, and E. Tiemann, Phys. Rev. A **87**, 050702(R) (2013).
[11] S. Dong, Y. Cui, C. Shen, Y. Wu, M. K. Tey, L. You, and B. Gao, Phys. Rev. A **94**, 062702 (2016).
[12] B. J. Sawyer, M. S. J. Horvath, E. Tiesinga, A. B. Deb, and N. Kjærgaard, Phys. Rev. A **96**, 022705 (2017).
[13] Y. Cui, C. Shen, M. Deng, S. Dong, C. Chen, R. Lü, B. Gao, M. K. Tey, and L. You, Phys. Rev. Lett. **119**, 203402 (2017).
[14] X.-C. Yao, R. Qi, X.-P. Liu, X.-Q. Wang, Y.-X. Wang, Y.-P. Wu, H.-Z. Chen, P. Zhang, H. Zhai, Y.-A. Chen *et al.*, Nat. Phys. **15**, 570 (2019).
[15] B. Zhu, S. Häfner, B. Tran, M. Gerken, J. Ulmanis, E. Tiemann, and M. Weidemüller, arXiv:1910.12011 [cond-mat.quant-gas].
[16] B. Zhu, S. Häfner, B. Tran, M. Gerken, J. Ulmanis, E. Tiemann, and M. Weidemüller (unpublished).
[17] S. Jochim, M. Bartenstein, A. Altmeyer, G. Hendl, C. Chin, J. H. Denschlag, and R. Grimm, Phys. Rev. Lett. **91**, 240402 (2003).
[18] M. W. Zwierlein, C. A. Stan, C. H. Schunck, S. M. F. Raupach, S. Gupta, Z. Hadzibabic, and W. Ketterle, Phys. Rev. Lett. **91**, 250401 (2003).
[19] M. Bartenstein, A. Altmeyer, S. Riedl, S. Jochim, C. Chin, J. H. Denschlag, and R. Grimm, Phys. Rev. Lett. **92**, 120401 (2004).
[20] C. Chin, M. Bartenstein, A. Altmeyer, S. Riedl, S. Jochim, J. H. Denschlag, and R. Grimm, Science **305**, 1128 (2004).
[21] T. Bourdel, L. Khaykovich, J. Cubizolles, J. Zhang, F. Chevy, M. Teichmann, L. Tarruell, S. J. J. M. F. Kokkelmans, and C. Salomon, Phys. Rev. Lett. **93**, 050401 (2004).
[22] M. W. Zwierlein, C. A. Stan, C. H. Schunck, S. M. F. Raupach, A. J. Kerman, and W. Ketterle, Phys. Rev. Lett. **92**, 120403 (2004).
[23] M. Bartenstein, A. Altmeyer, S. Riedl, S. Jochim, C. Chin, J. H. Denschlag, and R. Grimm, Phys. Rev. Lett. **92**, 203201 (2004).
[24] T. B. Ottenstein, T. Lompe, M. Kohnen, A. N. Wenz, and S. Jochim, Phys. Rev. Lett. **101**, 203202 (2008).
[25] J. H. Huckans, J. R. Williams, E. L. Hazlett, R. W. Stites, and K. M. O'Hara, Phys. Rev. Lett. **102**, 165302 (2009).
[26] A. N. Wenz, T. Lompe, T. B. Ottenstein, F. Serwane, G. Zürn, and S. Jochim, Phys. Rev. A **80**, 040702(R) (2009).
[27] J. R. Williams, E. L. Hazlett, J. H. Huckans, R. W. Stites, Y. Zhang, and K. M. O'Hara, Phys. Rev. Lett. **103**, 130404 (2009).
[28] T. Lompe, T. B. Ottenstein, F. Serwane, K. Viering, A. N. Wenz, G. Zürn, and S. Jochim, Phys. Rev. Lett. **105**, 103201 (2010).
[29] I. Ferrier-Barbut, M. Delehaye, S. Laurent, A. T. Grier, M. Pierce, B. S. Rem, F. Chevy, and C. Salomon, Science **345**, 1035 (2014).
[30] J. K. Chin, D. Miller, Y. Liu, C. Stan, W. Setiawan, C. Sanner, K. Xu, and W. Ketterle, Nature (London) **443**, 961 (2006).
[31] M. F. Parsons, F. Huber, A. Mazurenko, C. S. Chiu, W. Setiawan, K. Wooley-Brown, S. Blatt, and M. Greiner, Phys. Rev. Lett. **114**, 213002 (2015).
[32] P. M. Duarte, R. A. Hart, T.-L. Yang, X. Liu, T. Paiva, E. Khatami, R. T. Scalettar, N. Trivedi, and R. G. Hulet, Phys. Rev. Lett. **114**, 070403 (2015).
[33] A. Omran, M. Boll, T. A. Hilker, K. Kleinlein, G. Salomon, I. Bloch, and C. Gross, Phys. Rev. Lett. **115**, 263001 (2015).
[34] D. Greif, M. F. Parsons, A. Mazurenko, C. S. Chiu, S. Blatt, F. Huber, G. Ji, and M. Greiner, Science **351**, 953 (2016).
[35] D. Mitra, P. T. Brown, E. Guardado-Sanchez, S. S. Kondov, T. Devakul, D. A. Huse, P. Schauss, and W. S. Bakr, Nat. Phys. **14**, 173 (2018).
[36] F. Chevy, E. G. M. van Kempen, T. Bourdel, J. Zhang, L. Khaykovich, M. Teichmann, L. Tarruell, S. J. J. M. F. Kokkelmans, and C. Salomon, Phys. Rev. A **71**, 062710 (2005).
[37] J. Zhang, E. G. M. van Kempen, T. Bourdel, L. Khaykovich, J. Cubizolles, F. Chevy, M. Teichmann, L. Tarruell, S. J. J. M. F. Kokkelmans, and C. Salomon, Phys. Rev. A **70**, 030702(R) (2004).
[38] C. H. Schunck, M. W. Zwierlein, C. A. Stan, S. M. F. Raupach, W. Ketterle, A. Simoni, E. Tiesinga, C. J. Williams, and P. S. Julienne, Phys. Rev. A **71**, 045601 (2005).
[39] T. Nakasuji, J. Yoshida, and T. Mukaiyama, Phys. Rev. A **88**, 012710 (2013).
[40] J. Yoshida, T. Saito, M. Waseem, K. Hattori, and T. Mukaiyama, Phys. Rev. Lett. **120**, 133401 (2018).
[41] M. Waseem, T. Saito, J. Yoshida, and T. Mukaiyama, Phys. Rev. A **96**, 062704 (2017).
[42] M. Waseem, J. Yoshida, T. Saito, and T. Mukaiyama, Phys. Rev. A **98**, 020702(R) (2018).
[43] M. Waseem, Z. Zhang, J. Yoshida, K. Hattori, T. Saito, and T. Mukaiyama, J. Phys. B: At. Mol. Opt. Phys. **49**, 204001 (2016).

[44] J. Fuchs, C. Ticknor, P. Dyke, G. Veeravalli, E. Kuhnle, W. Rowlands, P. Hannaford, and C. J. Vale, Phys. Rev. A **77**, 053616 (2008).
[45] Y. Inada, M. Horikoshi, S. Nakajima, M. Kuwata-Gonokami, M. Ueda, and T. Mukaiyama, Phys. Rev. Lett. **101**, 100401 (2008).
[46] R. A. W. Maier, C. Marzok, C. Zimmermann, and P. W. Courteille, Phys. Rev. A **81**, 064701 (2010).
[47] R. Pires, J. Ulmanis, S. Häfner, M. Repp, A. Arias, E. D. Kuhnle, and M. Weidemüller, Phys. Rev. Lett. **112**, 250404 (2014).
[48] Due to the small splitting, as compared to the resonance widths, the peak positions and widths are strongly correlated in the fit near 185 G.
[49] S. Knoop, F. Ferlaino, M. Mark, M. Berninger, H. Schobel, H.-C. Nägerl, and R. Grimm, Nat. Phys. **5**, 227 (2009).
[50] L. Zhou and X. Cui, Phys. Rev. A **96**, 030701(R) (2017).
[51] S. S. Botelho and C. A. R. Sá de Melo, J. Low Temp. Phys. **140**, 409 (2005).
[52] V. Gurarie, L. Radzihovsky, and A. V. Andreev, Phys. Rev. Lett. **94**, 230403 (2005).
[53] C.-H. Cheng and S.-K. Yip, Phys. Rev. Lett. **95**, 070404 (2005).
[54] C. A. Regal, C. Ticknor, J. L. Bohn, and D. S. Jin, Phys. Rev. Lett. **90**, 053201 (2003).
[55] J. P. Gaebler, J. T. Stewart, J. L. Bohn, and D. S. Jin, Phys. Rev. Lett. **98**, 200403 (2007).
[56] K. Günter, T. Stöferle, H. Moritz, M. Köhl, and T. Esslinger, Phys. Rev. Lett. **95**, 230401 (2005).
[57] P. Peng, R. Zhang, L. Huang, D. Li, Z. Meng, P. Wang, H. Zhai, P. Zhang, and J. Zhang, Phys. Rev. A **97**, 012702 (2018).
[58] C. Luciuk, S. Trotzky, S. Smale, Z. Yu, S. Zhang, and J. H. Thywissen, Nat. Phys. **12**, 599 (2016).